# ALGORITHM THEORETICAL BASIS DOCUMENT: NET RADIOMETER

| PREPARED BY | ORGANIZATION | DATE |
|---|---|---|
| Derek Smith | FIU | 07/02/2013 |
| Josh Roberti | FIU | 07/17/2013 |

| APPROVALS (Name) | ORGANIZATION | APPROVAL DATE |
|---|---|---|
| David Tazik | CCB PROJ SCI | 08/18/2013 |
| Hanne Buur | CCB DIR SE | 08/27/2013 |
| | | |
| | | |

| RELEASED BY (Name) | ORGANIZATION | RELEASE DATE |
|---|---|---|
| Stephen Craft | SE | 08/28/2013 |

# CHANGE RECORD

| REVISION | DATE | ECO # | DESCRIPTION OF CHANGE |
|---|---|---|---|
| A | 08/28/2013 | ECO-00922 | Initial Release |
| | | | |

**TABLE OF CONTENTS**

**LIST OF TABLES AND FIGURES**

# 1 DESCRIPTION

Contained in this document are details concerning net radiation measurements made at all NEON sites. Long wave (LW) and short wave (SW) radiation, (both incoming and reflected) will be measured via the net radiometer discussed here. Specifically, the algorithm process necessary to convert "raw" sensor measurements into meaningful scientific units and their associated uncertainties are described.

## 1.1 Purpose

This document details the algorithms used for creating NEON Level 1 data product from Level 0 data, and ancillary data as defined in this document (such as calibration data), obtained via instrumental measurements made by the net radiometer. It includes a detailed discussion of measurement theory and implementation, appropriate theoretical background, data product provenance, quality assurance and control methods used, approximations and/or assumptions made, and a detailed exposition of uncertainty resulting in a cumulative reported uncertainty for this product.

## 1.2 Scope

The theoretical background and entire algorithmic process used to derive Level 1 data from Level 0 data for the net radiometer are described in this document. It is expected that the net radiometer employed at all NEON tower sites is the Hukseflux NR01 (NEON part number: 0300070002). This document does not provide computational implementation details, except for cases where these stem directly from algorithmic choices explained here.

# 2 RELATED DOCUMENTS AND ACRONYMS

## 2.1 Applicable Documents

| | | |
|---|---|---|
| AD[01] | NEON.DOC.000001 | NEON Observatory Design |
| AD[02] | NEON.DOC.005003 | NEON Scientific Data Products Catalog |
| AD[03] | NEON.DOC.005004 | NEON Level 1-3 Data Products Catalog |
| AD[04] | NEON.DOC.005005 | NEON Level 0 Data Products Catalog |
| AD[05] | NEON.DOC.000782 | NEON ATBD QA/QC data consistency |
| AD[06] | NEON.DOC.011081 | ATBD QA/QC plausibility tests |
| AD[07] | NEON.DOC.000783 | ATBD QA/QC Time Series Signal Despiking for TIS Level 1 Data Products |
| AD[08] | NEON.DOC.000802 | NR01 – Net Radiometer Calibration/Validation Procedure |
| AD[09] | NEON.DOC.000849 | $C^3$ Net Radiometer |
| AD[10] | NEON.DOC.000927 | NEON Calibration and Sensor Uncertainty Values |
| AD[11] | NEON.DOC.000785 | TIS Level 1 Data Products Uncertainty Budget Estimation Plan |
| AD[12] | NEON.DOC.000751 | CVAL Transfer of standard procedure |
| AD[13] | NEON.DOC.000746 | Evaluating Uncertainty (CVAL) |
| AD[14] | NEON.DOC.002002 | Engineering Master Location Sensor Matrix |
| AD[15] | NEON.DOC.001113 | Quality Flags and Quality Metrics for TIS Data Products |

## 2.2 Reference Documents

| | | |
|---|---|---|
| RD[01] | NEON.DOC.000008 | NEON Acronym List |
| RD[02] | NEON.DOC.000243 | NEON Glossary of Terms |

## 2.3 Acronyms

| Acronym | Explanation |
|---|---|
| ATBD | Algorithm Theoretical Basis Document |
| CVAL | NEON Calibration, Validation, and Audit Laboratory |
| DAS | Data Acquisition System |
| DP | Data Product |
| L0 | Level 0 |
| L1 | Level 1 |
| PRT | Platinum Resistance Thermometer |
| UQ | Unquantifiable Uncertainty |

## 2.4 Verb Convention

"Shall" is used whenever a specification expresses a provision that is binding. The verbs "should" and "may" express non-mandatory provisions. "Will" is used to express a declaration of purpose on the part of the design activity.

# 3 DATA PRODUCT DESCRIPTION

## 3.1 Variables Reported

Table 1 details the net radiometer-related L1 DPs provided by the algorithms documented in this ATBD.

**Table 1.** List of net radiometer-related L1 DPs that are produced in this ATBD.

| Data product | Averaging Period | Units | Data Product ID |
|---|---|---|---|
| **Tower Sensor** | | | |
| 1-minute Mean Incoming Shortwave Radiation (*Mean_IS₁*) | 1-min | $W\ m^{-2}$ | NEON.DXX.XXX.DP1.00023.001.001.001.001 |
| 1-minute Minimum Incoming Shortwave Radiation ($Min\_IS_1$) | 1-min | $W\ m^{-2}$ | NEON.DXX.XXX.DP1.00023.001.002.001.001 |
| 1-minute Maximum Incoming Shortwave Radiation ($Max\_IS_1$) | 1-min | $W\ m^{-2}$ | NEON.DXX.XXX.DP1.00023.001.003.001.001 |
| 1-minute Incoming Shortwave Variance ($\sigma^2\_IS_1$) | 1-min | $(W\ m^{-2})^2$ | NEON.DXX.XXX.DP1.00023.001.004.001.001 |
| 1-minute Incoming Shortwave QA/QC Summary ($Qsum\_IS_1$) | 1-min | Text | NEON.DXX.XXX.DP1.00023.001.005.001.001 |
| 1-minute Incoming Shortwave QA/QC Report ($Qrpt\_IS_1$) | 1-min | Text | NEON.DXX.XXX.DP1.00023.001.006.001.001 |
| 30-minute Mean Incoming Shortwave Radiation ($Mean\_IS_{30}$) | 30-min | $W\ m^{-2}$ | NEON.DXX.XXX.DP1.00023.001.001.001.002 |
| 30-minute Minimum Incoming Shortwave Radiation ($Min\_IS_{30}$) | 30-min | $W\ m^{-2}$ | NEON.DXX.XXX.DP1.00023.001.002.001.002 |
| 30-minute Maximum Incoming Shortwave Radiation ($Max\_IS_{30}$) | 30-min | $W\ m^{-2}$ | NEON.DXX.XXX.DP1.00023.001.003.001.002 |
| 30-minute Incoming Shortwave Variance ($\sigma^2\_IS_{30}$) | 30-min | $(W\ m^{-2})^2$ | NEON.DXX.XXX.DP1.00023.001.004.001.002 |
| 30-minute Incoming Shortwave QA/QC Summary ($Qsum\_IS_{30}$) | 30-min | Text | NEON.DXX.XXX.DP1.00023.001.005.001.002 |
| 1-minute Mean Reflected Shortwave Radiation ($Mean\_RS_1$) | 1-min | $W\ m^{-2}$ | NEON.DXX.XXX.DP1.00023.001.007.001.001 |
| 1-minute Minimum Reflected Shortwave Radiation ($Min\_RS_1$) | 1-min | $W\ m^{-2}$ | NEON.DXX.XXX.DP1.00023.001.008.001.001 |
| 1-minute Maximum Reflected | 1-min | $W\ m^{-2}$ | NEON.DXX.XXX.DP1.00023.001.009.001.001 |

| | | | |
|---|---|---|---|
| Shortwave Radiation (*$Max\_RS_1$*) | | | |
| 1-minute Reflected Shortwave Variance ($\sigma^2\_RS_1$) | 1-min | $(W\ m^{-2})^2$ | NEON.DXX.XXX.DP1.00023.001.010.001.001 |
| 1-minute Reflected Shortwave QA/QC Summary ($Qsum\_RS_1$) | 1-min | Text | NEON.DXX.XXX.DP1.00023.001.011.001.001 |
| 1-minute Reflected Shortwave QA/QC Report ($Qrpt\_RS_1$) | 1-min | Text | NEON.DXX.XXX.DP1.00023.001.012.001.001 |
| 30-minute Mean Reflected Shortwave Radiation ($Mean\_RS_{30}$) | 30-min | $W\ m^{-2}$ | NEON.DXX.XXX.DP1.00023.001.007.001.002 |
| 30-minute Minimum Reflected Shortwave Radiation ($Min\_RS_{30}$) | 30-min | $W\ m^{-2}$ | NEON.DXX.XXX.DP1.00023.001.008.001.002 |
| 30-minute Maximum Reflected Shortwave Radiation ($Max\_RS_{30}$) | 30-min | $W\ m^{-2}$ | NEON.DXX.XXX.DP1.00023.001.009.001.002 |
| 30-minute Reflected Shortwave Variance ($\sigma^2\_RS_{30}$) | 30-min | $(W\ m^{-2})^2$ | NEON.DXX.XXX.DP1.00023.001.010.001.002 |
| 30-minute Reflected Shortwave QA/QC Summary ($Qsum\_RS_{30}$) | 30-min | Text | NEON.DXX.XXX.DP1.00023.001.011.001.002 |
| 1-minute Mean Incoming Longwave Radiation ($Mean\_IL_{1min}$) | 1-min | $W\ m^{-2}$ | NEON.DXX.XXX.DP1.00023.001.013.001.001 |
| 1-minute Minimum Incoming Longwave Radiation ($Min\_IL_1$) | 1-min | $W\ m^{-2}$ | NEON.DXX.XXX.DP1.00023.001.014.001.001 |
| 1-minute Maximum Incoming Longwave Radiation ($Max\_IL_1$) | 1-min | $W\ m^{-2}$ | NEON.DXX.XXX.DP1.00023.001.015.001.001 |
| 1-minute Incoming Longwave Variance ($\sigma^2\_IL_1$) | 1-min | $(W\ m^{-2})^2$ | NEON.DXX.XXX.DP1.00023.001.016.001.001 |
| 1-minute Incoming Longwave QA/QC Summary ($Qsum\_IL_1$) | 1-min | Text | NEON.DXX.XXX.DP1.00023.001.017.001.001 |
| 1-minute Incoming Longwave QA/QC Report ($Qrpt\_IL_1$) | 1-min | Text | NEON.DXX.XXX.DP1.00023.001.018.001.001 |
| 30-minute Mean Incoming Longwave Radiation ($Mean\_IL_{30}$) | 30-min | $W\ m^{-2}$ | NEON.DXX.XXX.DP1.00023.001.013.001.002 |
| 30-minute Minimum Incoming Longwave Radiation ($Min\_IL_{30}$) | 30-min | $W\ m^{-2}$ | NEON.DXX.XXX.DP1.00023.001.014.001.002 |
| 30-minute Maximum Incoming Longwave Radiation ($Max\_IL_{30}$) | 30-min | $W\ m^{-2}$ | NEON.DXX.XXX.DP1.00023.001.015.001.002 |
| 30-minute Incoming Longwave Variance ($\sigma^2\_IL_{30}$) | 30-min | $(W\ m^{-2})^2$ | NEON.DXX.XXX.DP1.00023.001.016.001.002 |
| 30-minute Incoming Longwave QA/QC Summary ($Qsum\_IL_{30}$) | 30-min | Text | NEON.DXX.XXX.DP1.00023.001.017.001.002 |
| 1-minute Mean Reflected Longwave Radiation ($Mean\_RL_{1min}$) | 1-min | $W\ m^{-2}$ | NEON.DXX.XXX.DP1.00023.001.019.001.001 |
| 1-minute Minimum Reflected Longwave Radiation ($Min\_RL_1$) | 1-min | $W\ m^{-2}$ | NEON.DXX.XXX.DP1.00023.001.020.001.001 |

| | | | |
|---|---|---|---|
| 1-minute Maximum Reflected Longwave Radiation (*Max_RL*$_1$) | 1-min | $W\ m^{-2}$ | NEON.DXX.XXX.DP1.00023.001.021.001.001 |
| 1-minute Reflected Longwave Variance ($\sigma^2$_*RL*$_1$) | 1-min | $(W\ m^{-2})^2$ | NEON.DXX.XXX.DP1.00023.001.022.001.001 |
| 1-minute Reflected Longwave QA/QC Summary (*Qsum_RL*$_1$) | 1-min | Text | NEON.DXX.XXX.DP1.00023.001.023.001.001 |
| 1-minute Reflected Longwave QA/QC Report (*Qrpt_RL*$_1$) | 1-min | Text | NEON.DXX.XXX.DP1.00023.001.024.001.001 |
| 30-minute Mean Reflected Longwave Radiation (*Mean_RL*$_{30}$) | 30-min | $W\ m^{-2}$ | NEON.DXX.XXX.DP1.00023.001.019.001.002 |
| 30-minute Minimum Reflected Longwave Radiation (*Min_RL*$_{30}$) | 30-min | $W\ m^{-2}$ | NEON.DXX.XXX.DP1.00023.001.020.001.002 |
| 30-minute Maximum Reflected Longwave Radiation (*Max_RL*$_{30}$) | 30-min | $W\ m^{-2}$ | NEON.DXX.XXX.DP1.00023.001.021.001.002 |
| 30-minute Reflected Longwave Variance ($\sigma^2$_*RL*$_{30}$) | 30-min | $(W\ m^{-2})^2$ | NEON.DXX.XXX.DP1.00023.001.022.001.002 |
| 30-minute Reflected Longwave QA/QC Summary (*Qsum_RL*$_{30}$) | 30-min | Text | NEON.DXX.XXX.DP1.00023.001.023.001.002 |
| **Soil Array Sensor** | | | |
| 1-minute Mean Incoming Longwave Radiation (*Mean_IL*$_{1min}$) | 1-min | $W\ m^{-2}$ | NEON.DXX.XXX.DP1.00023.001.013.002.001 |
| 1-minute Minimum Incoming Longwave Radiation (*Min_IL*$_1$) | 1-min | $W\ m^{-2}$ | NEON.DXX.XXX.DP1.00023.001.014.002.001 |
| 1-minute Maximum Incoming Longwave Radiation (*Max_IL*$_1$) | 1-min | $W\ m^{-2}$ | NEON.DXX.XXX.DP1.00023.001.015.002.001 |
| 1-minute Incoming Longwave Variance ($\sigma^2$_*IL*$_1$) | 1-min | $(W\ m^{-2})^2$ | NEON.DXX.XXX.DP1.00023.001.016.002.001 |
| 1-minute Incoming Longwave QA/QC Summary (*Qsum_IL*$_1$) | 1-min | Text | NEON.DXX.XXX.DP1.00023.001.017.002.001 |
| 1-minute Incoming Longwave QA/QC Report (*Qrpt_IL*$_1$) | 1-min | Text | NEON.DXX.XXX.DP1.00023.001.018.002.001 |
| 30-minute Mean Incoming Longwave Radiation (*Mean_IL*$_{30}$) | 30-min | $W\ m^{-2}$ | NEON.DXX.XXX.DP1.00023.001.013.002.002 |
| 30-minute Minimum Incoming Longwave Radiation (*Min_IL*$_{30}$) | 30-min | $W\ m^{-2}$ | NEON.DXX.XXX.DP1.00023.001.014.002.002 |
| 30-minute Maximum Incoming Longwave Radiation (*Max_IL*$_{30}$) | 30-min | $W\ m^{-2}$ | NEON.DXX.XXX.DP1.00023.001.015.002.002 |
| 30-minute Incoming Longwave Variance ($\sigma^2$_*IL*$_{30}$) | 30-min | $(W\ m^{-2})^2$ | NEON.DXX.XXX.DP1.00023.001.016.002.002 |
| 30-minute Incoming Longwave QA/QC Summary (*Qsum_IL*$_{30}$) | 30-min | Text | NEON.DXX.XXX.DP1.00023.001.017.002.002 |
| 1-minute Mean Reflected Longwave Radiation (*Mean_RL*$_{1min}$) | 1-min | $W\ m^{-2}$ | NEON.DXX.XXX.DP1.00023.001.019.002.001 |

| | | | |
|---|---|---|---|
| 1-minute Minimum Reflected Longwave Radiation ($Min\_RL_1$) | 1-min | $W\ m^{-2}$ | NEON.DXX.XXX.DP1.00023.001.020.002.001 |
| 1-minute Maximum Reflected Longwave Radiation ($Max\_RL_1$) | 1-min | $W\ m^{-2}$ | NEON.DXX.XXX.DP1.00023.001.021.002.001 |
| 1-minute Reflected Longwave Variance ($\sigma^2\_RL_1$) | 1-min | $(W\ m^{-2})^2$ | NEON.DXX.XXX.DP1.00023.001.022.002.001 |
| 1-minute Reflected Longwave QA/QC Summary ($Qsum\_RL_1$) | 1-min | Text | NEON.DXX.XXX.DP1.00023.001.023.002.001 |
| 1-minute Reflected Longwave QA/QC Report ($Qrpt\_RL_1$) | 1-min | Text | NEON.DXX.XXX.DP1.00023.001.024.002.001 |
| 30-minute Mean Reflected Longwave Radiation ($Mean\_RL_{30}$) | 30-min | $W\ m^{-2}$ | NEON.DXX.XXX.DP1.00023.001.019.002.002 |
| 30-minute Minimum Reflected Longwave Radiation ($Min\_RL_{30}$) | 30-min | $W\ m^{-2}$ | NEON.DXX.XXX.DP1.00023.001.020.002.002 |
| 30-minute Maximum Reflected Longwave Radiation ($Max\_RL_{30}$) | 30-min | $W\ m^{-2}$ | NEON.DXX.XXX.DP1.00023.001.021.002.002 |
| 30-minute Reflected Longwave Variance ($\sigma^2\_RL_{30}$) | 30-min | $(W\ m^{-2})^2$ | NEON.DXX.XXX.DP1.00023.001.022.002.002 |
| 30-minute Reflected Longwave QA/QC Summary ($Qsum\_RL_{30}$) | 30-min | Text | NEON.DXX.XXX.DP1.00023.001.023.002.002 |

### 3.2 Input Dependencies

Table 2 details the net radiometer-related L0 DPs used to produce L1 DPs via this ATBD.

**Table 2.** List of net radiometer-related L0 DPs that are transformed into L1 DPs via this ATBD.

| Data product | Sample Frequency | Units | Data Product ID |
|---|---|---|---|
| | | **Tower Sensor** | |
| Upward facing pyranometer ($P_u$) | 1 Hz | *V* | NEON.DXX.XXX.DP0.00023.001.001.001.001.001 |
| Downward facing pyranometer ($P_d$) | 1 Hz | *V* | NEON.DXX.XXX.DP0.00023.001.002.001.001.001 |
| Upward facing pyrgeometer ($U_u$) | 1 Hz | *V* | NEON.DXX.XXX.DP0.00023.001.003.001.001.001 |
| Downward facing pyrgeometer ($U_d$) | 1 Hz | *V* | NEON.DXX.XXX.DP0.00023.001.004.001.001.001 |
| Sensor body PRT resistance at temperature *T* ($R_t$) | 1 Hz | *Ω* | NEON.DXX.XXX.DP0.00023.001.005.001.001.001 |
| Heater Flag ($QF_H$) | 1 Hz | *NA* | NEON.DXX.XXX.DP0.00023.001.006.001.001.001 |
| | | **Soil Array Sensor** | |
| Upward facing pyrgeometer ($U_u$) | 1 Hz | *V* | NEON.DXX.XXX.DP0.00023.001.003.002.000.001 |
| Downward facing pyrgeometer ($U_d$) | 1 Hz | *V* | NEON.DXX.XXX.DP0.00023.001.004.002.000.001 |
| Sensor body PRT resistance at temperature *T* ($R_t$) | 1 Hz | *Ω* | NEON.DXX.XXX.DP0.00023.001.005.002.000.001 |
| Heater Flag ($QF_H$) | 1 Hz | *NA* | NEON.DXX.XXX.DP0.00023.001.006.002.000.001 |

### 3.3 Product Instances

A Hukseflux NR01 will be deployed on all core and re-locatable towers. Additionally, a Hukseflux NR01 will be deployed in the central most plot of the soil array at all tower sites, which will measure *only* incoming and reflected LW radiation at the soil surface.

### 3.4 Temporal Resolution and Extent

One- and thirty-minute averages of SW and LW radiation will be calculated to form L1 DPs.

### 3.5 Spatial Resolution and Extent

Net radiometers will be deployed at the top level of the tower infrastructure and the central most plot of the soil array at all core and re-locatable tower sites. Thus, NR01 measurements will represent the point in space where the measurement is taken. See AD[14] for site specific sensor location details.

## 4 SCIENTIFIC CONTEXT

The sun's energy is emitted to the earth mainly in the form of incoming short-wave (SW) radiation, with a small portion of it falling into incoming LW radiation wavelengths. Approximately 50% of the sun's emitted energy lies in the infrared wavelengths, between 0.7 and 5 µm. Of the remaining radiant energy from the sun, around 40% can be found in the visible region (i.e. 0.4-0.7 µm) and 10% in the ultraviolet region (i.e. <0.4 µm) (Fu, 2003; Goody and Yung, 1995).

A fraction of incoming solar radiation is returned to space through either reflection or backscattering, which is known as albedo. The earth's albedo is presently around 31% (Fu, 2003). Thus, the bulk of the sun's radiation is absorbed by the earth's surface. A portion of the radiation absorbed by the earth is then re-emitted back into the atmosphere in the form of LW radiation. This re-emitted LW radiation can be absorbed by gases in the atmosphere and re-radiated back to the earth's surface. This re-radiation of LW radiation results in atmospheric warming, known as the greenhouse effect. As such, incoming and reflected SW and LW radiation are principal drivers of the hydrologic and energy budgets. Thus, time-series studies of net radiation are of great interest to the scientific and broader community to understand rates of change and their potential implications.

### 4.1 Theory of Measurement

The Hukseflux NR01 is a passive net radiation sensor, which serves to measure four separate components of surface radiation. The radiometer uses thermopiles to determine SW and LW fluxes from small output voltages that are proportional to the incoming and reflected SW and LW fluxes. The net radiometer consists of four main components; a pyranometer, pyrgeometer, PRT, and a heater.

The pyranometer is used to measure SW radiation flux ($300 < \lambda < 2800$ nm), and is composed of one upward and one downward facing thermopile to measure incoming and reflected SW radiation. The thermopile in the pyranometer is encased in a glass dome, which limits the spectral response from 300 to 2800 nm and shields the thermopile from atmospheric convection. The pyrgeometer determines LW radiation flux in the range of $4500 < \lambda < 50000$ nm. One pyrgeometer will face upward and determine incoming LW radiation, while the other pyrgeometer will face the earth's surface and measure reflected LW radiation. The pyrgeometer's thermopile is enclosed by a silicon window to inhibit radiation below 4500nm from entering and to shield the thermopile from atmospheric convection.

The pyrgeometer sensor itself emits LW radiation. Thus, the pyrgeometer's thermopile measurements are composed of the incoming minus the sensor reflected LW radiation. If we consider the sensor to be a black body, we apply the Stefan–Boltzmann law to determine the portion of LW radiation emitted by the sensor. To summarize, the Stefan–Boltzmann law states that radiation emitted by a black body object is directly proportional to the fourth power of the black body's temperature. A PRT housed in the sensor body will determine sensor body temperature. Thus, the PRT will allow the fraction of LW radiation emitted by the pyrgeometer to be measured. The last component of the net radiometer is a heater, which is used to prevent condensation from developing on the sensor.

### 4.2 Theory of Algorithm

In addition to the thermopile outputs from the upward and downward facing pyranometers and pyrgeometers, sensor specific sensitivities are needed to derive values for SW and LW radiation. The sensor specific sensitivities are determined by CVAL according to AD[08]. As previously mentioned, sensor body temperature is needed to determine incoming and reflected LW radiation. This is due to the LW radiation that is emitted by the pyrgeometer, and thus the thermopile measurements represent incoming minus the portion of LW radiation that is emitted. Sensor body temperature will be determined from the PRT using two separate equations; one equation for temperatures < 0 °C, Eq. (2), and one for temperatures ≥ 0 °C, Eq. (3), (ASTM, 2004). The raw resistance received from the PRT will identify which equation will be used to determine the temperature (*T*) accordingly:

$$T = \begin{vmatrix} \text{Eq. (2)} & \text{if} & (\mathrm{R_t} < 100\ \Omega) \\ \text{Eq. (3)} & \text{if} & (\mathrm{R_t} \geq 100\ \Omega) \end{vmatrix} \tag{1}$$

The non-linearity of a PRT can be expressed as follows for resistance < 100 [Ω] as (ASTM, 2004):

$$T_i = \sum_{k=1}^{4} D_k \left( R_{t_i}/R_0 - 1 \right)^k \tag{2}$$

Where:

$T_i$ = Individual (1 Hz) Temperature (°C)
$R_{t_i}$ = Individual PRT resistance at temperature, *T* (Ω)
$R_0$ = 100 (Ω) [Nominal resistance at 0 °C defined as 100 Ω for a PRT 100]

$D_1$ = 255.819 (°C) [coefficient defined by ASTM – E 1137/E 1137M]
$D_2$ = 9.14550 (°C) [coefficient defined by ASTM – E 1137/E 1137M]
$D_3$ = -2.92363 (°C) [coefficient defined by ASTM – E 1137/E 1137M]
$D_4$ = 1.79090 (°C) [coefficient defined by ASTM – E 1137/E 1137M]

Likewise, for resistance ≥ 100 [Ω] ASTM (2004) expresses PRTs' non-linearity as:

$$T_i = \frac{\left(A^2 - 4B\left(1 - R_{t_i}/R_0\right)\right)^{\frac{1}{2}} - A}{2B} \qquad (3)$$

Where:

$T_i$ = Individual (1 Hz) Temperature (°C)
$R_{t_i}$ = Individual PRT resistance at temperature, *T* (Ω)
$R_0$ = 100 (Ω) [Nominal resistance at 0°C defined as 100 Ω for a PRT 100]
$A$ = $3.9083*10^{-3}$ ($°C^{-1}$) [coefficient defined by IEC 751 and the ITS-90 scale]
$B$ = $-5.775*10^{-7}$ ($°C^{-2}$) [coefficient defined by IEC 751 and the ITS-90 scale]

Note: In the event that the International Temperature Scale (ITS) is updated from the ITS-90 scale, the coefficients listed above will be revised to reflect the most current ITS.

It is then necessary to convert temperature from Celsius to Kelvin as follows:

$$T(K) = T(°\mathrm{C}) + 273.15\ \mathrm{K} \qquad (4)$$

Once sensor body temperature is resolved, individual, incoming and reflected LW radiation is determined accordingly (NREL 2013):

$$L_{I_i} = \alpha_{u0} + \alpha_{u1}U_{u_i} + \alpha_{u2}\sigma_{SB}\left(T_i + cU_{u_i}\right)^4 \qquad (5)$$

And

$$L_{R_i} = \alpha_{d0} + \alpha_{d1}U_{d_i} + \alpha_{d2}\sigma_{SB}\left(T_i + cU_{d_i}\right)^4 \qquad (6)$$

Where:

$L_{I_i}$ = Individual (1 Hz) incoming Long Wave Radiation [$W\ m^{-2}$]
$L_{R_i}$ = Individual reflected Long Wave Radiation [$W\ m^{-2}$]
$U_{u_i}$ = Individual upward- facing pyrgeometer [*V*]
$U_{d_i}$ = Individual downward- facing pyrgeometer [*V*]
$\alpha_{u0}$ = Upward facing pyrgeometer sensor sensitivity [$W\ m^{-2}$ ] *provided by CVAL*

$\alpha_{u1}$ = Upward facing pyrgeometer sensor sensitivity [$W\,m^{-2}\,V^{-1}$] *provided by CVAL*
$\alpha_{u2}$ = Upward facing pyrgeometer sensor sensitivity [*unitless*] *provided by CVAL*
$\alpha_{d0}$ = Downward facing pyrgeometer sensor sensitivity [$W\,m^{-2}$] *provided by CVAL*
$\alpha_{d1}$ = Downward facing pyrgeometer sensor sensitivity [$W\,m^{-2}\,V^{-1}$] *provided by CVAL*
$\alpha_{d2}$ = Downward facing pyrgeometer sensor sensitivity [*unitless*] *provided by CVAL*
$\sigma_{SB}$ = $5.67*10^{-8}$ [Stefan-Boltzmann constant, $W\,m^{-2}K^{-4}$]
$T_i$ = Sensor body temperature [$K$]
$c$ = 704.4 [$K\,V^{-1}$]

Incoming and reflected SW radiation is determined from the pyranometer as follows:

$$S_{I_i} = P_{u_i}\beta_u \qquad (7)$$

and

$$S_{R_i} = P_{d_i}\beta_d \qquad (8)$$

Where:

$S_{I_i}$ = Incoming Short Wave Radiation ($W\,m^{-2}$)
$S_{R_i}$ = Reflected Short Wave Radiation ($W\,m^{-2}$)
$P_{u_i}$ = Upward facing pyranometer ($V$)
$P_{d_i}$ = Downward facing pyranometer ($V$)
$\beta_u$ = Upward facing pyranometer sensor sensitivity ($W\,m^{-2}\,V^{-1}$) *Provided by CVAL*
$\beta_d$ = Downward facing pyranometer sensor sensitivity ($W\,m^{-2}\,V^{-1}$) *Provided by CVAL*

One-minute and thirty-minute averages will be determined accordingly to create L1 DPs. Here we let $Rad$ represent incoming and reflected LW and SW radiation since they will be averaged the same way:

$$\overline{Rad}_1 = \frac{1}{n}\sum_{i=x}^{n} Rad_i \qquad (9)$$

where, for each minute average, *n* is the number of measurements in the averaging period T and the averaging period is defined as 0 ≤ T < 60 seconds.

and

$$\overline{Rad}_{30} = \frac{1}{n}\sum_{i=x}^{n} Rad_i \qquad (10)$$

where, for each thirty-minute average, *n* is the number of measurements in the averaging period T and averaging periods are defined as 0 ≤ T < 1800 seconds.

Note: The beginning of the first averaging period in a series shall be the nearest whole minute less than or equal to the first timestamp in the series.

## 5 ALGORITHM IMPLEMENTATION

Data flow for signal processing of L1 DPs will be treated in the following order.

1. The net radiometer L0 DPs will be converted into incoming and reflected SW and LW radiation through Eq. (1)-(8).
2. QA/QC Plausibility tests will be applied to the data stream in accordance with AD[06], details are provided below.
3. Signal despiking and time series analysis will be applied to the data stream in accordance with AD[07].
4. One- and thirty-minute SW and LW radiation averages will be calculated using Eq. (9) and (10) and descriptive statistics, i.e. minimum, maximum, and variance, will be determined for averaging periods.
5. QA/QC consistency tests will be applied to one- and thirty-minute averages in accordance with AD[05].
6. QA/QC summary (*Qsum*) will be produced for one- and thirty-minute averages according to AD[15].

<u>**QA/QC Procedure**</u>:

1. **Plausibility Tests** AD[08] – All plausibility tests will be determined for the net radiometer. Test parameters will be provided by FIU and maintained in the CI data store. All plausibility tests will be applied to the sensor's converted L0 DPs and an associated quality flags (QFs) will be generated for each test.

2. **Sensor Test** – A heater flag as identified in the $C^3$ document (AD[09]) will be applied to L0 DPs while the heater is operational. It is assumed that any heater-induced temperature changes in the sensor will be in equilibrium with the PRT. Therefore, any measurement variability induced by the heater, while it is on, will be accounted for by the internal PRT. The heater flag will be combined with the other quality flags to form the L1 QA/QC summary. This offers a user greater transparency, as one will be able to identify the number of L0 DPs where the heater was on that went into creating the L1 DP.

3. **Signal Despiking and Time Series Analysis** – Time segments and threshold values for the automated despiking QA/QC routine will be specified by FIU and maintained in the CI data store. Flags from the despiking analysis will be applied according to AD[07].

4. **Consistency Analysis** – Currently, there is no plan to run consistency analysis on the L1 DP for the net radiometer. However, time series consistency analysis may be explored in the future.

5. **Quality Flags (QFs) and Quality Metrics (QMs)** AD[15] – If a datum has one of the following flags it will not be used to create a L1 DP, $\underline{QF_R}$ and $\underline{QF_D}$. α and β QFs and QMs will be determined for the following flags $QF_R$, $QF_\sigma$, $QF_\delta$, $QF_S$, $QF_N$, $QF_G$, and $QF_D$. All L1 DPs will have an associated final quality flag, $QF_{NEON}$, and quality summary, Qsum, as detailed in AD[15]. Flags that may be associated with measurements from the net radiometer, as well as information maintained in the CI data store can be found below in Tables 3 and 4.

**Table 3.** Flags associated with net radiometer measurements.

| **Tests** | **Flags** |
|---|---|
| Range | $QF_R$ |
| Sigma (σ) | $QF_\sigma$ |
| Delta (δ) | $QF_\delta$ |
| Step | $QF_S$ |
| Null | $QF_N$ |
| Gap | $QF_G$ |
| Signal Despiking and Time Series Analysis | $QF_D$<br>$QF_o$<br>$QF_I$ |
| Sensor Test (Heater Flag) AD[09] | $QF_H$<br>$QF_F$ |
| Final quality flag | $QF_{NEON}$ |

**Table 4.** Information maintained in the CI data store for the net radiometer.

| Tests/Values | CI Data Store Contents |
|---|---|
| Range | Minimum and maximum values |
| Sigma (σ) | Time segments and threshold values |
| Delta (δ) | Time segment and threshold values |
| Step | Threshold values |
| Null | Test limit |
| Gap | Test limit |
| Signal Despiking and Time Series Analysis | Time segments and threshold values |
| Calibration | AD[08] |
| Uncertainty | AD[10] |
| Sensor Test | AD[09] |
| Final Quality Flag | AD[15] |

# 6 UNCERTAINTY

Uncertainty of measurement is inevitable (JCGM 2008, 2012; Taylor 1997). It is crucial that uncertainties are identified and quantified to determine statistical interpretations about mean quantity and variance structure; both are important when constructing higher level data products (e.g., L1 DP) and modeled processes. This portion of the document serves to identify, evaluate, and quantify sources of uncertainty relating to L1 mean DPs. It is a reflection of the information described in AD[11], and is explicitly described for the net radiometer assembly in the following sections.

## 6.1 Uncertainty of Radiation Measurements

Uncertainty of the net radiometer assembly is discussed in this section. Sources of uncertainties include those arising from the calibration procedure, pyranometer, pyrgeometer, Body temperature, heater, and noise from the DAS (Figure 1).

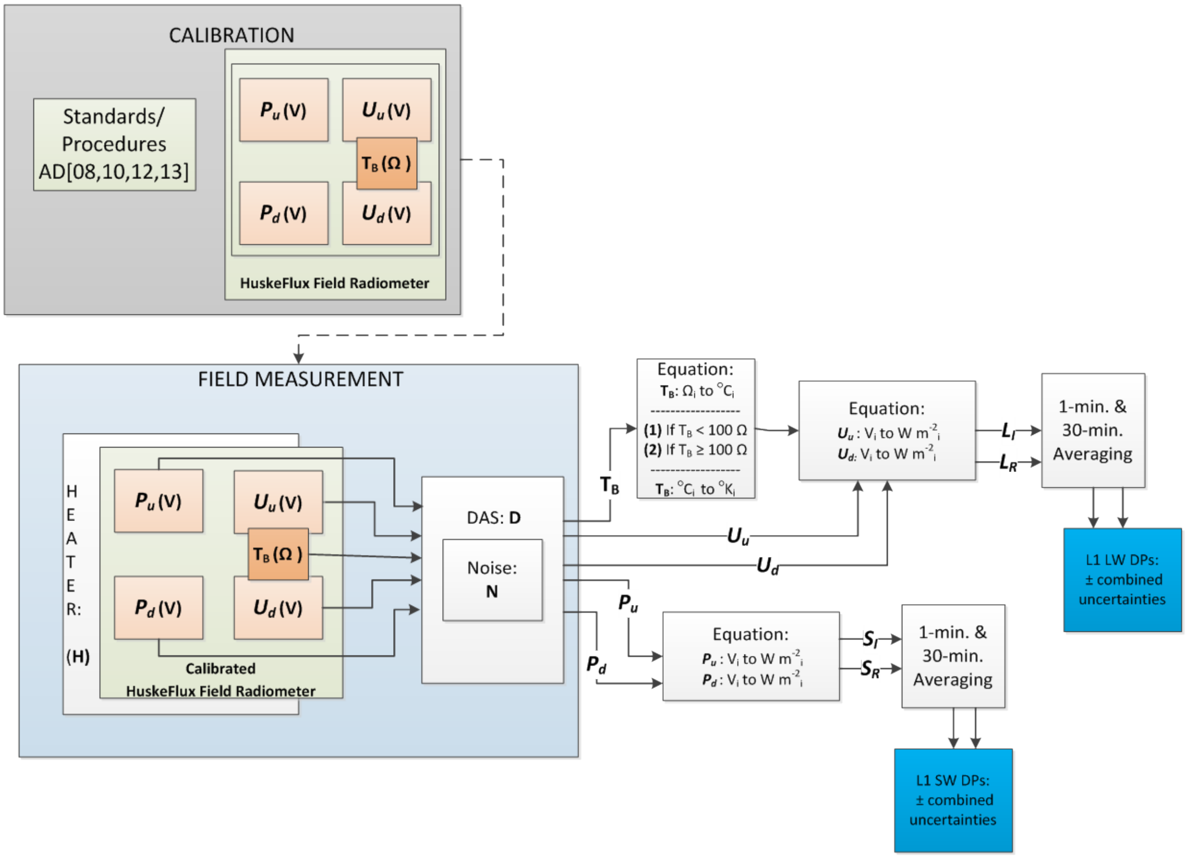


**Figure 1:** Displays the data flow and associated uncertainties of L1 DPs. Salmon colored boxes represent direct measurement of incoming /outgoing radiation based on the theory of passive radiation sensors. For a detailed explanation of the net radiometer calibration procedures please refer to AD[08,10,12,13].

### 6.1.1 Calibration

Uncertainties associated with net radiometers and their calibration processes are combined into a standard uncertainty $u_c(X_{Y_{CVAL}})$ by CVAL. This combined uncertainty represents i) the variation of an individual sensor from the mean of a sensor population, ii) uncertainty of the calibration procedures and iii) uncertainty of coefficients used to convert raw signals to calibrated radiation (refer to Eq. (5) through (8)). It is a constant value that will be provided by CVAL (AD[10]), stored in the CI data store, and applied to all radiation measurements (that is, it does not vary with any specific sensor, DAS component, etc.).

**Notes:**

- *X* represents either SW or LW radiation, and subscript *Y* denotes either incoming or reflected radiation.
- Internal body temperature will not be calibrated by NEON's CVAL, thus, CVAL will not supply an uncertainty value for this measurement. Please refer to Section 6.1.3 for further justification.

### 6.1.2 DAS

To quantify DAS noise, *relative* uncertainty values, $u_r(\mathrm{V}_{DAS})$ (radiation measurements) and $u_r(\mathrm{R}_{DAS})$ (internal body temperature), will be provided by CVAL (AD[10]) and stored in the CI data store. These values must be converted into *standard* uncertainty values:

$$u(\mathrm{V}_{DAS_i}) = (u_r(\mathrm{V}_{DAS}) * V_i) + O_{DAS_v} \quad [V] \tag{11}$$

And

$$u(\mathrm{R}_{DAS_i}) = (u_r(\mathrm{R}_{DAS}) * R_i) + O_{DAS_R} \quad [\Omega] \tag{12}$$

Where $u(\mathrm{V}_{DAS_i})$ and $u(\mathrm{R}_{DAS_i})$ are the standard uncertainties of an *individual,* raw, voltage ($V_i$) and resistance ($R_i$) measurements, respectively. $O_{DAS}$ is the offset imposed by the DAS. The offset accounts for readings of 0.00 $[V] or$ $[\Omega]$; the offset values will be provided by CVAL (AD[10]) and maintained in the CI data store.

To calculate the partial uncertainty of individual *longwave* radiation measurements resulting from DAS noise, standard DAS uncertainties must be multiplied by the absolute value of Eq. (5)'s (incoming) or (6)'s (reflected) partial derivative with respect to the raw voltage measurement:

$$\frac{\partial L_{Y_i}}{\partial U_i} = \alpha_1 + 4c\alpha_2\sigma_{SB}(T_i + cU_i)^3 \tag{13}$$

$$u_U(L_{Y_i}) = \left|\frac{\partial L_{Y_i}}{\partial U_i}\right| u(U_i) \quad [W\ m^{-2}] \tag{14}$$

Where, $u(U_i) \equiv u(\mathrm{V}_{DAS_i})$; subscript *Y* denotes incoming or reflected radiation

The previous can be completed for individual *shortwave* radiation measurements by multiplying DAS uncertainties by the absolute value of Eq. (7)'s (incoming) or (8)'s (reflected) partial derivative with respect to the raw voltage measurement:

$$\frac{\partial S_{Y_i}}{\partial P_i} = \beta \tag{15}$$

$$u_P(S_{Y_i}) = \left|\frac{\partial S_{Y_i}}{\partial P_i}\right| u(P_i) \quad [W\ m^{-2}] \tag{16}$$

Where, $u(P_i) \equiv u(\mathrm{V}_{DAS_i})$; subscript *Y* denotes incoming or reflected radiation

Similarly, this can be calculated for the individual body temperature measurements. In the event that $R_{T_i} < 100\ [\Omega]$, the partial derivative of Eq. (2) with respect to the raw resistance measurement is computed:

***CASE 1***

$$\frac{\partial T_i}{\partial R_{T_i}} = \frac{D_1(R_0-1)^3 + R_{T_i}\left(2D_2(R_0-1)^2 + R_{T_i}\left(3D_3(R_0-1) + 4D_4R_{T_i}\right)\right)}{(R_0-1)^4} \quad (17)$$

If $R_{T_i} \geq 100\ [\Omega]$, the partial derivative of Eq. (3) with respect to the raw resistance measurement is computed:

***CASE 2***

$$\frac{\partial T_i}{\partial R_{T_i}} = \frac{1}{R_0\left(A^2 - 4B(1-\frac{R_{T_i}}{R_0})\right)^{\frac{1}{2}}} \quad (18)$$

And the absolute value of the appropriate resulting value is then multiplied by the uncertainty due to DAS noise:

$$u_{R_T}(T_i) = \left|\frac{\partial T_i}{\partial R_{T_i}}\right| u\left(R_{T_i}\right) \quad [K] \quad (19)$$

Where, $u(R_{T_i}) \equiv u(\mathrm{R}_{DAS_i})$

**Note:** Given that Eq. (19) represents uncertainty, its value can be given in $[K]$ without converting (scaling) from [°C] to $[K]$ via Eq. (4).

### 6.1.3 Body Temperature

To account for the long wave radiation emitted by the pyrgeometer, the body temperature of the pyrgeometer is calculated (Hukseflux 2007). Since the NR01's PRT is internal, it will not be directly calibrated by CVAL (as noted in Section 6.1.1). However, given that CVAL *will* calibrate the pyrgeometer and that LW radiation is a function of body temperature, the uncertainty of converting from [Ω] to [°C] using Eq. (2) and (3) is essentially quantified by CVAL during calibration of the pyrgeometer.

### 6.1.4 Heater

It is assumed that any heater-induced temperature changes in the sensor will be in equilibrium with the PRT. Therefore, any measurement uncertainty induced by the heater, should in theory be accounted for by the body temperature of the sensor.

### 6.1.5 Longwave radiation

The combined uncertainty for individual Longwave radiation measurements can be computed with the aid of the following equations. First, the sensitivity coefficient of longwave radiation must be derived with respect to the sensor's body temperature:

$$\frac{\partial L_{Y_i}}{\partial T_i} = 4\alpha_2\sigma_{SB}(T_i + cU_i)^3 \tag{20}$$

The absolute value of this sensitivity coefficient is then multiplied by the combined uncertainty of the individual body temperature measurement, i.e., the resulting value from Eq. (19):

$$u_T(L_{Y_i}) = \left|\frac{\partial L_{Y_i}}{\partial T_i}\right| u_{R_T}(T_i) \quad [W\ m^{-2}] \tag{21}$$

**Note regarding derivatives:** Since the uncertainty of converting from $[\Omega]$ to $[°C]$ or $[K]$ is quantified by CVAL as part of the pyrgeometer's calibration process (refer to Section 6.1.3), only the uncertainty introduced by the DAS, $u(R_{T_i})$, propagates with $T_i$ to Eq. (20). To promote brevity of individual equations, the partial derivative of Eq. (2) or (3) (depending on the magnitude of $R_{T_i}$) with respect to $R_{T_i}$ is quantified first. The absolute value of this derivative is then multiplied by the uncertainty of $R_{T_i}$. Lastly, the resulting value is then multiplied by the partial derivative of Eq. (20) with respect to $T_i$. Thus, Eq. (21) essentially exhibits the partial uncertainty of $L_{Y_i}$ as a function of $R_{T_i}$, i.e., $u_T(L_{Y_i}) \equiv u_{R_T}(L_{Y_i})$.

This value, along with the resulting value from Eq. (14) and the uncertainty provided by CVAL are then summed in quadrature:

$$u_c(L_{Y_i}) = \left(u^2(L_{Y_{CVAL}}) + u_U{}^2(L_{Y_i}) + u_T{}^2(L_{Y_i})\right)^{\frac{1}{2}} \quad [W\ m^{-2}] \tag{22}$$

Where, subscript Y represents either incoming or reflected radiation.

#### 6.1.6 Shortwave radiation

The combined uncertainty for individual shortwave radiation measurements is given below.

$$u_c(S_{Y_i}) = \left(u^2(S_{Y\,CVAL}) + u_P{}^2(S_{Y_i})\right)^{\frac{1}{2}} \quad [W\ m^{-2}] \tag{23}$$

Where, subscript Y represents either incoming or reflected radiation.

### 6.2 Combined Uncertainty – Level 1 Data Products

The L1 combined uncertainty is derived in a few steps. First, the resulting combined uncertainty of the individual radiation measurement is multiplied by the partial derivative of the L1 DP. Since the DP is a temporal average, the partial derivative with respect to an individual measurement is simply:

$$\frac{\partial \overline{X_Y}}{\partial X_{Y_i}} = \frac{1}{n} \tag{24}$$

Where $n$ represents the number of valid observations made during the averaging period. The absolute value of Eq. (24) is then multiplied by either Eq. (22) (LW radiation) or Eq. (23) (SW radiation):

$$u_{X_{Y_i}}(\overline{X_Y}) = \left|\frac{\partial \overline{X_Y}}{\partial X_{Y_i}}\right| u_c(X_{Y_i}) \quad [W\ m^{-2}] \tag{25}$$

Finally, the combined uncertainty of the L1 mean DP is calculated via quadrature:

$$u_c(\overline{X_Y}) = \left(\sum_{i=1}^{n} u_{X_{Y_i}}(\overline{X_Y})\right)^{\frac{1}{2}} \quad [W\ m^{-2}] \tag{26}$$

Where, *X* represents either SW or LW radiation, and subscript *Y* denotes either incoming or reflected radiation.

## 6.3 Expanded Uncertainty – Level 1 Data Products

The expanded uncertainty for the L1 mean radiation DPs can be derived in a few steps.

**Longwave Radiation:**

First, the effective degrees of freedom for 1 Hz longwave radiation are computed:

$$V_{eff\,L_{Y_i}} = \frac{{u_c}^4(L_{Y_i})}{\frac{u^4(L_{Y\,CVAL})}{Veff_{L_{Y\,CVAL}}} + \frac{{u_U}^4(L_{Y_i})}{Veff_{V_{DAS}}} + \frac{{u_T}^4(L_{Y_i})}{Veff_{R_{DAS}}}} \quad (27)$$

Where, $Veff_{L_{Y\,CVAL}}$, $Veff_{V_{DAS}}$, and $Veff_{R_{DAS}}$ are functions of the calibration process – their values will be stored provided by CVAL (AD[10]) and stored in the CI data store.

**Shortwave Radiation:**

The effective degrees of freedom for 1 Hz shortwave radiation are computed:

$$V_{eff\,S_{Y_i}} = \frac{{u_c}^4(S_{Y_i})}{\frac{u^4(L_{Y\,CVAL})}{Veff_{L_{Y\,CVAL}}} + \frac{{u_U}^4(L_{Y_i})}{Veff_{V_{DAS}}}} \quad (28)$$

**L1 Radiation (LW and SW):**

Upon computation of Eq. (27) (LW radiation) and Eq. (28) (SW radiation), the effective degrees of freedom for the L1 mean radiation DP can be computed:

$$V_{eff\,\overline{X_Y}} = \frac{{u_c}^4(\overline{X_Y})}{\sum_{i=1}^{n}\left(\frac{(u_c(X_{Y_i})/n)^4}{V_{eff\,X_{Y_i}}}\right)} \quad (29)$$

Where, *X* represents either SW or LW radiation, and subscript *Y* denotes either incoming or reflected radiation

Finally, the expanded uncertainty of the respective radiation DP is calculated:

$$U_{95}(\overline{X_Y}) = k_{95} * u_c(\overline{X_Y}) \quad [W\ m^{-2}] \tag{30}$$

Where $k_{95}$ is the coverage factor obtained with the aid of:

- Table 5 from AD[11]
- $V_{eff_{\overline{X_Y}}}$

### 6.4 Uncertainty Budget

The uncertainty budget is a visual aid detailing i) quantifiable sources of uncertainty, ii) means by which they are derived, and iii) the order of their propagation. Individual uncertainty values denoted in this budget are either provided here (within this document) or will be provided by other NEON teams (e.g., CVAL) and stored in the CI data store.

**Table 5:** Uncertainty budget for L1 mean radiation DPs. Shaded rows denote the order of uncertainty propagation (from lightest to darkest).

| **Source of uncertainty** | **Standard uncertainty component $u(x_i)$** | **Value of standard uncertainty [W m$^{-2}$]** | $c_i \equiv \frac{\partial f}{\partial x_i}$ | $u_i(Y) \equiv \lvert c_i \rvert u(x_i)$ **[W m$^{-2}$]** | **Degrees of Freedom** |
|---|---|---|---|---|---|
| L1 LW DP | $u_c(\overline{L_Y})$ | Eq. (26) | -- | -- | Eq. (29) |
| 1 Hz LW | $u_c(L_{Y_i})$ | Eq. (22) | Eq. (24) | Eq. (25) | Eq. (27) |
| Sensor/calibration | $u_c(L_{Y_{CVAL}})$ | AD[10] | 1 | AD[10] | AD[10] |
| Noise (DAS) | $u(U_i)$ | Eq. (11) [V] | Eq. (13) | Eq. (14) | AD[10] |
| Body temperature | $u_{R_T}(T_i)$ | Eq. (19) [K] | Eq. (20) | Eq. (21) | AD[10] |
| Noise (DAS) *CASE 1* | $u(R_{T_i})$ | Eq. (12) [Ω] | Eq. (17) | Eq. (19) [K] | AD[10] |
| Noise (DAS) *CASE 2* | $u(R_{T_i})$ | Eq. (12) [Ω] | Eq. (18) | Eq. (19) [K] | AD[10] |
| ______________ | __________ | __________ | ______ | ______________ | ______ |
| L1 SW DP | $u_c(\overline{S_Y})$ | Eq. (26) | -- | -- | Eq. (29) |
| 1 Hz SW | $u_c(S_{Y_i})$ | Eq. (23) | Eq. (24) | Eq. (25) | Eq. (28) |
| Sensor/calibration | $u_c(L_{Y_{CVAL}})$ | AD[10] | 1 | AD[10] | AD[10] |
| Noise (DAS) | $u(U_i)$ | Eq. (11) [V] | Eq. (15) | Eq. (16) | AD[10] |
| $k_{95}$: $v_{eff_{\overline{X_Y}}}$ & Table 5 of AD[11]<br>$U_{95}(\overline{X_Y})$: Eq. (30) | | | | | |

## 7 FUTURE PLANS AND MODIFICATIONS

Future system flags may be incorporated into the data stream and included in the QA/QC summary DP ($Qsum_{1min}$ and $Qsum_{30min}$) that summarizes any flagged data that went into the computation of the L1 DP.

## 8 BIBLIOGRAPHY

ASTM. (2004) Standard Specification for Industrial Platinum Resistance Thermometers. *ASTM International* pp. 7 DOI: 10.1520/E1137_E1137M-04

Campbell Scientific. (20082008) NR018) NR01 four-component net radiation sensor. *Campbell Scientific, Inc.*, pp. 404040404040.

Fu, Qiang. (2003). Encyclopedia of atmospheric sciences: radiation (solar). Elsevier. pp. 1859-1863. ISBN-10: 0122270908

Goody, R.M. and Y. L. Yung. (1995). Atmospheric radiation: theoretical basis. Oxford University Press. 2nd Ed. pp. 544. ISBN-10: 0195102916

Hukseflux. (2007) NR01 RA01 manual version 0715. *Hukseflux Thermal Sensors.* pp. 40

Joint Committee for Guides in Metrology (JCGM) (2008) Evaluation of measurement data – Guide to the expression of uncertainty in measurement. pp. 120.

JCGM (2012) International vocabulary of metrology – Basic and general concepts and associated terms (VIM). 3rd Edition. pp. 92

National Renewable Energy Laboratory (NREL) (2013) Pyrgeometer Calibration for DOE – Atmospheric System Research Program Using NREL Method. [Available online at : http://www.nrel.gov/docs/fy10osti/47756.pdf]

Taylor, J. R. (1997) An Introduction to Error Analysis: The Study of Uncertainties in Physical Measurements. University Science Books, Mill Valley, California. 2nd Ed. pp. 327.